

RESEARCH ARTICLE

Open Access



Photonitration of pyrene adsorbed on silica gel with NO₂

Kiyoshi Hasegawa^{1*}, Reona Mabuchi¹ and Shigehiro Kagaya¹

Abstract

To examine the heterogeneous photonitration of pyrene with NO₂ (approximately 0.2 ppm) on a heavy-traffic road, we studied the photonitration of pyrene adsorbed (pyrene_{ads}) on silica gel, which was used as SiO₂ in particulate matter (PM), with NO₂ (10.2, 2.0, and 0.20 ppm) under the atmospheric concentration ratio of pyrene_{ads} to NO₂ and compared the results with those obtained in the dark. The effects of irradiation, wavelength, and oxygen concentration in a NO₂ diluent on the photonitration were examined using a fluidized-bed column irradiated with simulated or real sunlight. Under the UV-light absorption of pyrene, the concentration of pyrene decreased exponentially in accordance with a pseudo-first-order reaction, while in the dark, it decreased sigmoidally in accordance with a H⁺-autocatalyzed reaction. The distribution and the yields of formed nitration products and their photooxidation products were affected by the light intensity, concentrations of NO₂, and oxygen in the NO₂ diluent. In the photonitration experiments using a high-pressure mercury lamp, formed 1-nitropyrene and minor dinitropyrenes were decreased by the transformation into their photooxidation products. Under 8-h exposure of pyrene to 10.2-ppm NO₂, the yield of 1-nitropyrene was 42% in N₂ and 28% in air. The oxygen inhibitory effect can be explained by the energy transfer from ¹pyrene* to oxygen. Radical cation intermediate (pyrene^{•+}-NO₂⁻) was proposed for 1-nitropyrene formation. Under 24-h exposure of pyrene to 2.0-ppm NO₂, the yields of 1-nitropyrene and the photooxidation products were 21.6% and 8.0%, respectively, in N₂ and 4.9% and 3.8%, respectively, in air. Under 24-h exposure of pyrene to 0.20-ppm NO₂, which is two times the 1-h NO₂ standard in the USA and China, the yields of 1-nitropyrene and the photooxidation products were 2.3% and 3.4%, respectively, in N₂ and 2.1% and 0.9%, respectively, in air. The significant decrease in the yields of 1-nitropyrene and the photooxidation products under the concentration of 0.20-ppm NO₂ can be explained by their easy photodecomposition with the increase in the photolysis of pyrene. Under the concentration of 0.20-ppm NO₂ in air, which is approximately the concentration on heavy-traffic roads, the decay rate of pyrene by the photonitration was increased by own photolysis, although the photonitration was inhibited by oxygen in air.

Keywords Pyrene, Silica gel, NO₂, Photonitration, Photolysis, Kinetics and mechanism, Concentration effects of NO₂ and pyrene

1 Introduction

Keyte et al. (2013) summarized the formation of mutagenic nitropolycyclic aromatic hydrocarbons (NPAHs) by the reaction of polycyclic aromatic hydrocarbons (PAHs) adsorbed on PM with NO₂; however, the effect of light irradiation has not been investigated under atmospheric concentrations of NO₂ and PAH adsorbed (PAH_{ads}) on PM. Seasonal and downwind sampling of PM showed that considerable amounts of NPAHs and oxygenated

*Correspondence:

Kiyoshi Hasegawa
hase4139@chive.ocn.ne.jp

¹ Department of Environmental Applied Chemistry, Faculty of Engineering, University of Toyama, 3190 Gofuku, Toyama 930-8555, Japan

PAHs were secondarily formed by the photochemical reactions of PAHs on urban PM (Kojima et al., 2010; Lin et al., 2015; Ma et al., 2016; Zhuo et al., 2017) and during atmospheric transport of PAH-adsorbed PM (Eiguren-Fernandez et al., 2008). To investigate the secondary transformation of the PAHs, it is necessary to study the photonitration and photooxidation of the PAHs under the polluted atmospheric concentrations of NO_2 and PAHs_{ads} (representative average concentrations of pyrene on PM in winter: $20 \text{ pg } \mu\text{g}^{-1}$, Noto Peninsula, Japan, Tang et al., 2015, and $206 \text{ pg } \mu\text{g}^{-1}$, Beijing, China, Lin et al., 2015); however, previous studies (Wu & Niki, 1985; Inazu et al., 1997; Cochran et al., 2016; Guan et al., 2017) were carried out under one to two orders of higher concentrations of NO_2 and PAHs_{ads} than those in the polluted atmosphere, except for the experiment by Sugiyama et al. (2001) using 0.2-ppm NO_2 , and gave no special consideration to the concentrations of PAHs_{ads} and NO_2 .

Wu and Niki (1985) reported the reactions between NO_2 (≥ 25 ppm) and pyrene adsorbed on silica plates in a N_2 or O_2/N_2 diluent using fluorescence spectroscopy, showing that pyrene decay followed a first-order kinetics with NO_2 concentration and was inhibited by O_2 in diluent gas. Inazu et al. (1997) studied the heterogeneous photoreaction of fluoranthene adsorbed on oxide particles with NO_2 (10 ppm) in a N_2 or air diluent and reported the distribution of resulting nitrofluoranthene, the formation mechanism of major 2-nitrofluoranthene, and its degradation with time. Although photoirradiation and oxygen promoted the degradation of fluoranthene, the structures of yellow degradation products were not identified because of insolubility in solvents. Sugiyama et al. (2001) studied the photonitration of pyrene adsorbed on metal oxides with NO_2 (0.2 ppm), showing that the yield of major 1-nitropyrene on silica gel for 2 h is 0.15%. Cochran et al. (2016) reported that UV irradiation of pyrene adsorbed on quartz filters in the presence of NO_2 (1–10 ppm) gave 1-nitropyrene; however, the yield was significantly lower than that without irradiation due to the photodegradation of 1-nitropyrene. Guan et al. (2017) reported that simulated sunlight enhanced the reactivity of PAHs adsorbed on soot with NO_2 (20–150 ppm); however, the yields of newly formed NPAHs were lower than those in the dark. These previous studies have not discussed the photonitration kinetics and mechanism based on products analyses.

The concentration of SiO_2 is high in inorganic particles in PM in large cities in the USA, Europe, and Asia (Harrison & Yin, 2000; Rodriguez et al., 2009; Gao et al., 2015). As silica gel has been selected because of its well-defined physical and chemical properties (Perraudin et al., 2005), a silica gel with a large surface area was used as SiO_2 in

PM to compare the photonitration of pyrene with the nitration of PAHs adsorbed on silica gel (Sugiyama et al., 2001; Wang et al., 1999; Hasegawa et al., 2020) and silica particles (Perraudin et al., 2005; Miet et al., 2009; Ma et al., 2011). The chemically synthesized silica gel and silica having a SiO_2 structure have been used as substrates for the nitration of PAHs (Sugiyama et al., 2001; Wang et al., 1999; Hasegawa et al., 2020; Perraudin et al., 2005; Miet et al., 2009; Ma et al., 2011) and their photolysis (Barbas et al., 1993; Mao & Thomas, 1994, 1995; Reyes et al., 2000) because the analysis of reactions on collected PM is complex, depending on the constituents. One-hour NO_2 standards in the USA and China are set at 0.10 ppm and $200 \text{ } \mu\text{g m}^{-3}$ (0.105 ppm), respectively. The US Environmental Protection Agency (EPA) has reported that NO_2 in heavy traffic or on freeways can be twice as high as levels measured in residential areas, and NO_2 concentrations may be 30 to 100% higher within approximately 50 m of heavy traffic/freeways, (United States Environmental Protection Agency (U. S. EPA), 2011). A meta-analysis of near-road NO_2 air pollution showed that about 17% NO_2 would be decreased at 100 m from the roads (Liu et al., 2019). Therefore, NO_2 (0.20 ppm), which can be observed on heavy-traffic roads, was used as the lowest NO_2 concentration. To understand the photonitration of pyrene with NO_2 under polluted atmosphere concentrations of pyrene_{ads} (20 pg on 1- μg silica gel) and NO_2 (0.20 ppm), we also studied the photonitration of pyrene adsorbed on silica gel with NO_2 (2.0 and 10.2 ppm) to facilitate the products analyses. The pyrene_{ads} was set to be proportional to the concentrations of NO_2 . The effects of light intensity, wavelength, and oxygen concentration in the NO_2 diluent on the photonitration of pyrene and the transformation products were investigated using a fluidized-bed column irradiated with simulated or real sunlight.

2 Materials and methods

2.1 Materials

Special-grade pyrene, 1-nitropyrene, 1,3-, 1,6-, and 1,8-dinitropyrenes, and 1,3-, 1,6-, and 1,8-pyrenedione were purchased from Wako Pure Chemical Industries, Ltd., Tokyo, Japan. Merck silica gel 60 (Art. 9385, 230–400 mesh, 0.040–0.063 mm, average pore diameter: 60 Å, surface area: $550 \text{ m}^2 \text{ g}^{-1}$, pH: 7) was used as a substrate. The silica gel was heated in an electric oven at 110–120 °C for 12 h. A certified NO_2 -loaded cylinder (10.2 ppm in N_2 or synthetic air, 20.1 ppm in N_2) was supplied by Takachiho Chemical Industry Inc., Tokyo, Japan, with 1-ppm NO_2 containing 2.50×10^{13} molecules cm^{-3} at 20 °C. NO_2 (2.0 and 0.20 ppm in N_2 or synthetic air) was prepared by diluting the NO_2 gas (10.2 ppm)

with N₂ or synthetic air using a flowmeter, and their concentrations were determined using the Saltzman method (Saltzman, 1960).

2.2 Adsorption of pyrene on silica gel

Three suspensions of (a) pyrene (5.00 mg) + silica gel (5.00 g) in 100-mL chloroform, (b) pyrene (4.90 mg) + silica gel (25.00 g) in 200-mL chloroform, and (c) pyrene (4.90 mg) + silica gel (250 g) in 500-mL chloroform were prepared. The pyrene_{ads} was set to be proportional to the concentrations of NO₂ (10.2, 2.0, and 0.20 ppm). After magnetically stirring three suspensions for 12 h, the chloroform was slowly evaporated at 35 °C under a weakly reduced pressure. After the pyrene-adsorbed particles were gradually dried in a vacuum desiccator with an aspirator, 15.0 mg (a), 75.0 mg (b), and 750.0 mg (c) aliquots of three samples were supersonically extracted with acetonitrile (25 mL). The concentrations of pyrene were measured using high-performance liquid chromatography (HPLC) at $\lambda = 234$ nm. The concentration of the pyrene_{ads} was determined by comparing the HPLC-measured areas of three extracts to that of a calibration curve of pyrene. The concentrations of pyrene were calculated to be 0.600 mg L⁻¹ (a) and 0.588 mg L⁻¹ (b and c) when 100% of the pyrene was adsorbed on the silica gel. As the adsorption ratio of pyrene was 95.0% (a), 93.9% (b), and 95.1% (c), silica gels adsorbing 950 pg μg^{-1} (a), 184 pg μg^{-1} (b), and 18.6 pg μg^{-1} (c) of pyrene were prepared. The surface coverage of pyrene (950 pg μg^{-1}) on silica gel (550 m² g⁻¹) was estimated 0.0067 because the cross section of the pyrene molecule was assumed to be 1.3 times that (1 nm²) of anthracene (Ma et al., 2011). This indicates that pyrene adsorbs on silica gel in a monolayer. The water content (H₂O_{ads}) of pyrene-adsorbed silica gel was gravimetrically determined to be in the range of 4.0–4.2 wt% as rehydration occurs in the work-up process. As the weight loss of the H₂O_{ads} on the pyrene-adsorbed silica gel was less than 0.1% after 5 days of storage in a desiccator kept at 3% humidity, the H₂O_{ads} is considered to be in adsorption equilibrium. Therefore, the H₂O_{ads} would not be decreased during the photonitration, although the humidity in the fluidized-bed reaction column was not measured when the pyrene-adsorbed silica gel is exposed to NO₂. The pyrene-adsorbed silica gel was stored in the dark to prevent the photodegradation of pyrene.

2.3 Photonitration

Pyrene was photonitrated by exposing NO₂ to pyrene_{ads} under three conditions: (a) NO₂ (10.2 ppm) + pyrene_{ads} (950 pg μg^{-1} , 4.70 $\mu\text{mol g}^{-1}$), (b) NO₂ (2.0 ppm) + pyrene_{ads} (184 pg μg^{-1} = 0.91 $\mu\text{mol g}^{-1}$), and (c) NO₂ (0.20 ppm) + pyrene_{ads} (18.6 pg μg^{-1} = 0.092 $\mu\text{mol g}^{-1}$).

2.4 Photoirradiation apparatus

Two fluidized-bed columns (Supplementary Materials Fig. S1) (Wang et al., 1999) irradiated by a 400-W high-pressure mercury lamp (UVL-400HA apparatus, Riko Co.) and a 500-W ultra-high-pressure mercury lamp (HX-500Q apparatus, WACOM Electric Co., Ltd.), with selectable irradiation wavelengths, were used separately. Both mercury lamps have emission lines of $\lambda = 302, 313, 334, 365, 405, 436, 546,$ and 578 nm. The latter irradiation apparatus is the same as that reported except that a reaction cell was replaced with a solution filter, and a chemical actinometer was removed (Hasegawa et al., 1998). The high-pressure mercury lamp and the ultra-high-pressure mercury lamp are hereafter denoted as the HP-Hg lamp and the UHP-Hg lamp, respectively. The three pyrene-adsorbed silica gels (1.00 g) were added to the three columns separately, and NO₂ (10.2, 2.0, and 0.20 ppm in N₂ or air) flowed through the bottom of the column at a flow rate of 400 mL min⁻¹ and 200 mL min⁻¹ for the HP-Hg lamp and the UHP-Hg lamp, respectively. The decrease in flow rate for the UHP-Hg lamp is due to the restriction of the irradiation area by a light flux 50 mm in diameter. The fluidized-bed column was set 16 cm away from the HP-Hg lamp and 6 cm away from the edge of the UHP-Hg lamp housing. Both Hg lamps were used as simulated sunlight; natural sunlight (from 7:30 to 15:30 in September 2002, Toyama, Japan) was also used.

The 400-W HP-Hg lamp was used to examine the effect of light intensity on the photoreaction of pyrene with NO₂. The light intensity was adjusted by surrounding the HP-Hg lamp with a thin aluminum plate drilled with different bore sizes. The transmittance (T) through the thin aluminum plates was measured with a UV spectrophotometer and found to be T = 21, 27, and 48%. Therefore, the irradiance on the fluidized-bed columns was 21, 27, and 48% that emitted from the HP-Hg lamp. The 500-W UHP-Hg lamp was used to examine the effects of wavelength and oxygen concentration in the dilution gas on the photoreaction of pyrene with NO₂. The collimated beam 50 mm in diameter was irradiated in parallel on wavelength-selective absorption filters. A Toshiba UV-D36A band-pass filter (300 nm < λ < 380 nm) and a Pyrex filter ($\lambda > 290$ nm) were used to select the light-absorption bands of pyrene (302, 313, and 334 nm). A solution filter (0.25 M NaNO₃ + 0.10 M NaNO₂, 1.5 cm thick) and a Pyrex filter ($\lambda > 290$ nm) were used to select the wavelength longer than 370 nm. The light intensities irradiated from two mercury lamps and sunlight were measured at the surface of the fluidized-bed column using an ultraviolet intensity meter (UV-M02, ORC Manufacturing Co. Ltd., Japan), which can measure the irradiance (mW/cm²) at the ranges of 241–271 nm (UV25, max: 250 nm), 320–390 nm (UV35, max: 350 nm), and 330–490 nm (UV42,

max: 420 nm). Experiments were also carried out without photoirradiation in a shaded draft.

2.5 Analysis

The NO_2 flow was stopped at an appropriate time, and 0.015 g of silica gel was taken out. Pyrene and products on silica gel were extracted with 5 mL of acetonitrile under ultrasonic irradiation under the photonitration condition (a). Under photonitration conditions (b) and (c), they were extracted with 5 mL (1 mL of the internal standard solution of chrysene: 0.025 mM in acetonitrile+4 mL of acetonitrile) and 2 mL (1 mL of the internal standard solution of chrysene: 0.0050 mM in acetonitrile+1 mL of acetonitrile) of acetonitrile solution under ultrasonic irradiation, respectively. These suspensions were centrifuged, and the supernatant solutions (extracts) were used for HPLC analyses. C_0 is the concentration of pyrene in the extract at 0 min, and C_t is the concentrations of pyrene and products in the extracts at t min or t (h), calculated using external standard calibration curves (experiment a) or internal standard calibration curves (experiments b and c) at 234 nm. Although an internal standard method was not used in the experiment (a), almost the same recoveries (C_0 /theoretical initial concentrations) for pyrene (97.1%) and 1-nitropyrene (96.4%) do not affect the ratios of C_t/C_0 . After exposure to NO_2 , the products on the silica gel remaining in the column were extracted with 5 mL of chloroform under ultrasonic irradiation. After centrifugation, the concentrated supernatant solution (extracts) was used for the analyses by gas chromatography (GC) and GC-mass spectrometry (GC-MS). GC and GC-MS analyses were repeated without adding the internal standard substance to the extracts. The HPLC, GC, and GC-MS instruments and analytical conditions are described in supporting materials. The experimental method of fluorescence quenching is described in supporting materials. Fluorescence spectra were recorded using a HITACHI 650-10S fluorescence spectrophotometer.

3 Results and discussion

3.1 Effects of light intensity, wavelength, and oxygen concentration in NO_2 diluent on the decay of pyrene

Figure 1 shows the effect of light intensity on the decay of pyrene by exposing NO_2 (10.2 ppm in N_2) under irradiation ($T=100\%$ and 21%) by the HP-Hg lamp with the decay of pyrene under sunlight and in the dark. Sunlight was used without adjusting the light intensity, although the sunlight irradiance on pyrene varied with time during the 8-h irradiation. The decay rate of pyrene increased as the light intensity increased. The decay rate of pyrene under light irradiation greatly contrasted with that in the dark, i.e., the pyrene decay proceeded exponentially

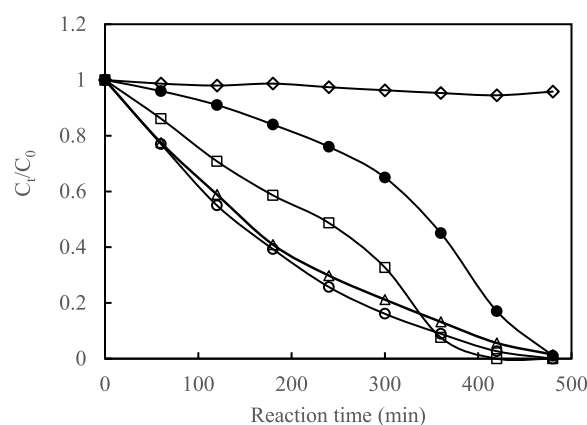


Fig. 1 Effect of light irradiation on the reaction of pyrene with 10.2-ppm NO_2 in N_2 (○, △, □, ●) and photolysis of pyrene in the absence of NO_2 (◇). HP-Hg lamp (○, ◇: $T=100\%$, □: $T=21\%$), sunlight (△), in the dark (●). Light irradiance of the HP-Hg lamp (mW cm^{-2}) at $T=100\%$: UV 25: 0.29, UV 35: 2.60, UV 42: 4.80, sunlight: UV 25: 0.20 (7:30), 0.75 (9:30), 1.20 (11:30), 1.21 (13:30), 0.51 (15:30), UV 35: 0.43 (7:30), 1.55 (9:30), 2.21 (11:30), 1.71 (13:30), 0.68 (15:30), UV 42: 1.43 (7:30), 5.61 (9:30), 8.09 (11:30), 6.52 (13:30), 2.60 (15:30)

under the HP-Hg light ($T=100\%$) and sunlight, while it proceeded sigmoidally in the dark as already reported for the H^+ -autocatalyzed reaction, in which the protons formed by the dissociation of HNO_3 started the nitration and the protons released by the formation of 1-nitropyrene acted as an autocatalyst to accelerate the nitration (Hasegawa et al., 2020). When pyrene was irradiated with 21% ($T=21\%$) of the light emitted from the HP-Hg lamp, it decayed exponentially before 180 min and sigmoidally after 180 min. These results indicate that the nitration mechanism of pyrene changes with light intensity. As the photolysis of pyrene was only 4.2% for 480 min under the irradiation condition of $T=100\%$ in the absence of NO_2 , the effect of the photolysis on the photonitration of pyrene with NO_2 is small. 1-Nitropyrene was obtained as a major product under light irradiation.

Figure S2 (supplementary materials) shows the relationship between $\ln(C_t/C_0)$ and reaction time under irradiation ($T=100\%$) by the HP-Hg lamp. As the decay deviated from the pseudo-first-order kinetics after 240 min, the observed rate constant (k_{obs}) was determined to be $9.0 \times 10^{-5} \text{ s}^{-1}$ for 240 min ($C_t/C_0=25.7\%$, which was 2.0 times greater than the k_{obs} ($4.6 \times 10^{-5} \text{ s}^{-1}$) in the rapid-decay range in the dark (Fig. 1), 5.3 times greater than the k_{obs} ($1.7 \times 10^{-5} \text{ s}^{-1}$) of pyrene on dry quartz with 3-ppm NO_2 in the dark (Kameda et al., 2016), and 3.0 times greater than the k_{obs} ($3 \times 10^{-5} \text{ s}^{-1}$) of pyrene on silica particles with 0.055-ppm NO_2 in the dark (Perraudin et al., 2005). This indicates that the nitration of pyrene adsorbed on silica gel was enhanced under light irradiation. The k_{obs} in the rapid decay range in the dark

was determined by drawing a tangent at the inflection time (350 min, $C_t/C_0=0.50$) as detailed in our previous report (Hasegawa et al., 2020).

Figure S3 (supplementary materials) shows the effect of wavelength on the nitration of pyrene with NO_2 (10.2 ppm in N_2) under irradiation by the UHP-Hg lamp. The flow rate of NO_2 was lowered from 400 (HP-Hg lamp) to 200 mL min^{-1} so that all suspended pyrene-adsorbed silica gels can be irradiated by the light flux. Pyrene decayed according to the pseudo-first-order kinetics under the irradiation of 300–380 nm, which involves absorption bands (302, 313, and 334 nm) of pyrene. Under irradiation longer than 370 nm, which pyrene does not absorb, the decay of pyrene was largely suppressed, and an induction period (420 min) was observed, although a sigmoidal curve was not observed due to the short reaction time. This result indicates that the photonitration under visible light proceeds via the H^+ -autocatalyzed nitration mechanism. Figure S4 (supplementary materials) shows the relationship between $\ln(C_t/C_0)$ and reaction time under the irradiation of 300–380 nm. As the decay deviated from the pseudo-first-order kinetics after 240 min, the k_{obs} was determined to be $6.0 \times 10^{-5} \text{ s}^{-1}$ for 240 min (C_t/C_0 40.5%). The deviation of pyrene decay from the pseudo-first-order kinetics in the final stage (Figs. S2 and S4) was also observed in the reaction of NO_2 with pyrene and anthracene adsorbed on silica gel (Hasegawa et al., 2020), with anthracene adsorbed on SiO_2 and MgO (Ma et al., 2011), and with pyrene adsorbed on clay minerals and Fe_2O_3 (Kameda et al., 2016). The causes are unclear at present.

Figure S5 shows the effect of oxygen concentration in the dilution gas on the reaction of pyrene with NO_2 (10.2 ppm) under irradiation ($\lambda=300\text{--}380 \text{ nm}$) by the UHP-Hg lamp. The pyrene decay decreases as the oxygen concentration increases, because oxygen quenches the photoexcited pyrene, which is discussed in supporting materials.

3.2 Effect of light intensity on the formation of 1-nitropyrene

Figure 2 shows the effect of light intensity on the formation of 1-nitropyrene under irradiation by the HP-Hg lamp with the photolysis of 1-nitropyrene in the absence of NO_2 . The concentration of 1-nitropyrene increased linearly for 60 min under the light intensity of $T=100\%$, 48%, 27%, and 21%. Under the light intensity of $T=100\%$ and 48%, the concentration of 1-nitropyrene exponentially increased between 60 and 360 min and then leveled off. Under the light intensity of $T=27\%$, it increased exponentially between 60 and 240 min and then gradually increased. Under the light intensity of $T=21\%$, it abruptly increased after 300 min via the exponential

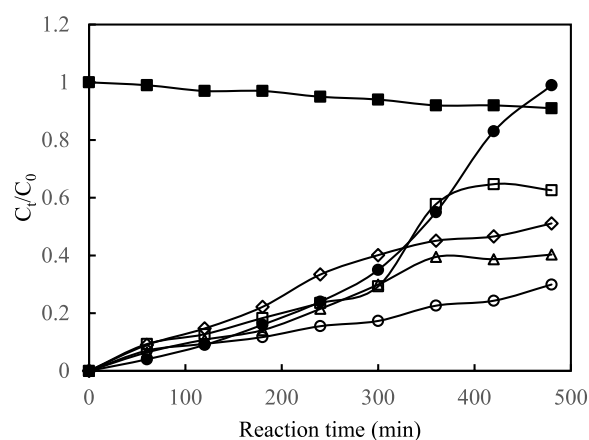


Fig. 2 Effect of light intensity on the formation of 1-nitropyrene (○, △, ◇, □) and the photolysis of 1-nitropyrene in the absence of NO_2 (■). NO_2 (10.2 ppm in N_2) and HP-Hg lamp ($T=100\%$). ○: $T=100\%$, △: $T=48\%$, ◇: $T=27\%$, □: $T=21\%$, ●: in the dark. Light irradiance (mW cm^{-2}) at $T=100\%$: UV 25: 0.29, UV 35: 2.60, UV 42: 4.80

increase in the concentration of 1-nitropyrene and then leveled off. The abrupt increase in the concentration of 1-nitropyrene is considered to be caused by the accelerated decay of pyrene between 300 and 360 min, as shown in Fig. 1 ($T=21\%$). The accelerated decay of pyrene is also observed after 300 min in the dark, as shown in Fig. 1. Therefore, the H^+ -autocatalyzed formation of 1-nitropyrene becomes dominant under weak light intensity. Figure 2 also suggests that the decay of 1-nitropyrene would occur in two stages: between 60 and 360 min and after 360 min. The yield of 1-nitropyrene is lower under any light intensity than that (99%) observed when pyrene was autocatalytically decayed in the dark (Hasegawa et al., 2020). It reached 63% ($T=21\%$), 51% ($T=27\%$), 46% ($T=48\%$), and 42% ($T=100\%$) at 480 min, indicating that the increase in light intensity decreases the yield of 1-nitropyrene. Under 480-min exposure of pyrene to 10.2-ppm NO_2 in air ($T=100\%$), the yield of 1-nitropyrene was 28%. As the photolysis decay of 1-nitropyrene was 10% for 480 min in the absence of NO_2 , the decrease in 1-nitropyrene is not ascribed to the photolysis of 1-nitropyrene.

3.3 Reaction products under light irradiation

Figure 3a–f shows the GC chromatograms of the extracts obtained by exposing NO_2 (10.2 ppm in N_2) to pyrene for 480 min under various irradiation conditions: (a) $T=21\%$, (b) $T=48\%$, (c) $300 \text{ nm} < \lambda < 380 \text{ nm}$ (absorption band of pyrene), (d) $\lambda > 370 \text{ nm}$, (e) sunlight, and (f): $T=100\%$. GC–MS measurement of the extracts (a–f) was also carried out. Table 1 shows the molecular and fragment ions of the products. The content (%) of the products, which was determined based on the peak areas of

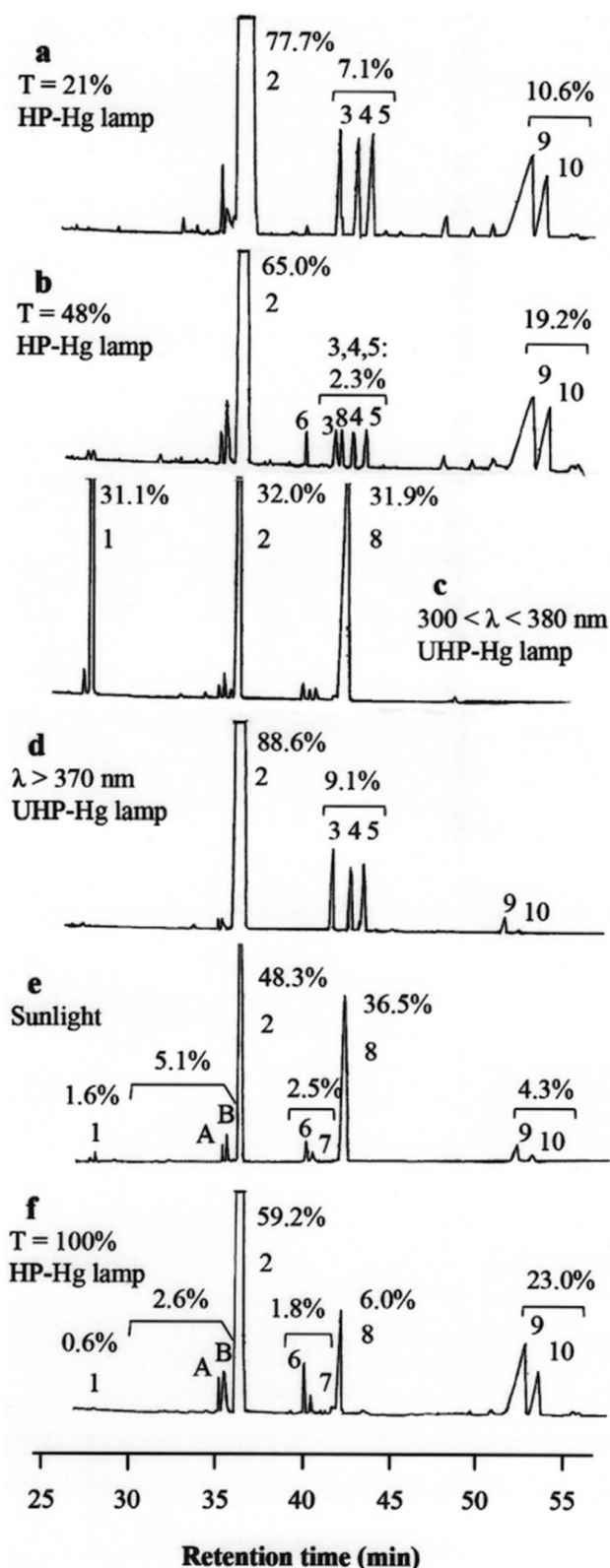


Fig. 3 GC chromatograms (a–f) of the extracts (a–f) obtained by exposing NO_2 (10.2 ppm in N_2) to pyrene for 480 min under various irradiation conditions

each GC chromatogram, is shown near the peaks. Product and product distribution changed depending upon the light intensity and wavelength. Pyrene (1), 1-nitropyrene (2), and 1,3- (3), 1,6- (4), and 1,8-dinitropyrenes (5) were observed with nitrated photooxidation products (6, 7, 8, 9, and 10) and the photooxidation products of 1. The structures of 2–5 were confirmed by matching the retention times and the mass spectra with those of the standard samples. Although 6–8 and 9–10 probably have pyrenedione skeletons with one and two NO_2 groups, respectively, from the MS fragmentation patterns, their structures could not be identified because a remaining oxygen-containing group is unclear. In the GC chromatogram of 3a, 2 and 3–5 are observed with 9 and 10. The total content of 3–5 decreased, and that of 9 and 10 increased as the light intensity increased from $T=21$ to 100% (Fig. 3a, b, and f). In Fig. 3b, the contents of 3–5 decreased, and the small amounts of 6 and 8 appeared, which already appeared as a shoulder peak of peak 3 in Fig. 3a. In the GC chromatograms of Fig. 3e and f, 3–5 are not observed, while new peaks (6–8) are observed with 2, 9, 10, and the small amounts of oxidation products (A, B) of 1. Under pyrene absorption light, 2 and 8 are observed (Fig. 3c), while under visible light irradiation, 2 is observed with the small amounts of 3–5 and trace amounts of 9 and 10 (Fig. 3d). The formation of 3–5 and 9 and 10, which were not formed in the dark reaction of 1 with NO_2 , is probably because 2.5% of the UHP-Hg light of 330 nm penetrated the solution filter. When the diluent of NO_2 was changed from N_2 to air under sunlight irradiation for 480 min, the contents of 1 increased and those of 2 and 6–10 decreased as follows: 1 (1.6% \rightarrow 49.3%), 2 (48.3% \rightarrow 42.7%), 6–8 (39.0% \rightarrow 5.3%), and 9–10 (4.3% \rightarrow 0%).

Figure S7 shows HPLC chromatograms of the extract a ($T=21\%$) to examine the time courses of 3–5, which are considered to be the precursors of 9 and 10. Nine and 10 increase after 120 min, and 6–8 increase after 360 min, while 3–5 are observed at 480 min in the elution order of 5, 4, and 3 before the peak of 2. These results indicate that the formation of 9 and 10 would proceed rapidly without accumulating 3–5, and they would be observed in the final slow-reaction period. The HPLC chromatograms of the extracts b and f showed that the peaks of 3–5 disappeared at 480 min, when the light intensity increased from $T=48$ to 100%.

In the GC–MS chromatograms of the extracts (e and f), two very small peaks of A1 and A2 (total yields: e, 0.8%; f, 0.4%) and B (yields: e, 4.3%; f, 2.2%) were observed before peak 2 at the following retention times: A1, 30.8 min; A2, 31.6 min; and B, 33.6 min. A1, A2, and B are assumed to be dihydroxy pyrenediones (A1), a photooxidation product of pyrenedione (A2), and dihydroxynitropyrene (B),

Table 1 Molecular and fragment ions of the products contained in the extracts (a–f) obtained under light irradiation

Extract	Peak	Product	M ⁺	Molecular and fragment ions
	2	1-Nitropyrene (2)	247	247 (M ⁺), 217 (M ⁺ -NO), 201 (M ⁺ -NO ₂)
	3	1,3-Dinitropyrene (3)	292	292 (M ⁺), 276 (M ⁺ -O), 262 (M ⁺ -NO)
	4	1,6-Dinitropyrene (4)	292	246 (M ⁺ -NO ₂), 232 (M ⁺ -2NO)
	5	1,8-Dinitropyrene (5)	292	216 (M ⁺ -NO ₂ -NO), 200 (M ⁺ -2NO ₂)
	6	Photooxidation products of 1-Nitropyrenedione (6, 7, 8)	291	291 (M ⁺), 275 (M ⁺ -O), 263 (M ⁺ -CO)
	7		291	261 (M ⁺ -NO), 245 (M ⁺ -NO ₂)
	8		291	233 (M ⁺ -CO-O), 217 (M ⁺ -CO-NO ₂)
	9	Photooxidation products of dinitropyrenedione (9, 10)	336	336 (M ⁺), 320 (M ⁺ -O), 308 (M ⁺ -CO)
	10		336	306 (M ⁺ -NO), 290 (M ⁺ -NO ₂)
				278 (M ⁺ -NO-CO), 262 (M ⁺ -NO ₂ -CO) 244 (M ⁺ -2NO ₂), 232 (M ⁺ -NO ₂ -CO-NO), 216 (M ⁺ -2NO ₂ -CO) 187 (M ⁺ -2NO ₂ -CO-CHO)
	A1	Dihydroxypyrenediones	264	264 (M ⁺), 246 (M ⁺ -H ₂ O), 218 (M ⁺ -H ₂ O-CO), 218 (M ⁺ -OH-CHO), 202 (M ⁺ -2OH-CO), 191 (M ⁺ -OH-2CO), 189 (M ⁺ -H ₂ O-CO-CHO)
	A2	Photooxidation product of pyrenedione	246	246 (M ⁺), 218 (M ⁺ -CO), 201 (M ⁺ -CO-OH), 189 (M ⁺ -CO-CHO)
	B	Dihydroxynitropyrene	279	279 (M ⁺), 261 (M ⁺ -H ₂ O), 247 (M ⁺ -2OH+2H), 232 (M ⁺ -H ₂ O-NO+H), 217 (M ⁺ -2OH-NO ₂ +2H), 201 (M ⁺ -2OH+2H-NO ₂), 189, 167, 149

as shown in Table 1; however, their structures could not be identified because standard and synthesized chemicals were not available. 1-Hydroxypyrene (Reyes et al., 2000; Garcia-Berrios & Arce, 2012), 1,6- and 1,8-pyrenediones (Reyes et al., 2000; Garcia-Berrios & Arce, 2012), and 1-hydroxy-x-nitropyrenes (Kameda, et al., 2011; Garcia-Berrios & Arce, 2012), which were formed by irradiating *I* on silica gel (Reyes et al., 2000) and *2* in organic solvents (Kameda, et al., 2011; Garcia-Berrios & Arce, 2012), were not observed because the photonitration of *1* and *2* became dominant over the photooxidation of *1* and *2*.

3.4 Time course of the products

Figure S8 (supplementary materials) shows the HPLC chromatograms of the extracts obtained every 60 min under irradiation by the HP-Hg lamp ($T=100\%$). The HPLC chromatograms obtained by 420-min and 480-min irradiation are similar after 10 min to the GC chromatogram (Fig. 3f) obtained by 480-min irradiation ($T=100\%$). The intensities of peaks 9 and 10 increase from 60 to 300 min, while the intensities of peaks 6–8 increase from 360 to 480 min with the decrease in 9 and 10. The dependence of appearance order of the products 9–10 and 6–8 on the light intensity described in Fig. 3 expects that peaks 9 and 10 appear before the appearance of peaks 6–8 under the light irradiation of $T=100\%$. Furthermore, three peaks of 6, 7, and 8, in which peaks 6 and 7 probably overlapped in the HPLC chromatograms, and two peaks of 9 and 10 are observed in both chromatograms of GC and HPLC.

The assignment of numbers to the five peaks was made according to the order of elution and similarity of the peak relative intensity to that of the peaks 6–10 in the GC chromatogram of Fig. 3f. Based on these observations, peaks 6–8 were regarded as the products 6, 7, and 8, and peaks 9 and 10 were regarded as the products 9 and 10. Peaks 1 and 2 were identified as *1* and *2* from the matching of the retention times with standard samples.

Figure 4 shows the time course of *1* and the products, where their response factors at 234 nm were regarded as the same. The formation rate of *2* decreases from the pseudo-first-order increase between 60 and 360 min with the increase in 9 and 10 (path A) and levels off with the increase in 6, 7, and 8 (path B). Products 3–5 were not observed under strong light irradiation ($T=100\%$) as shown in Fig. 3f. These results indicate that the photonitration of pyrene would proceed via the paths A and B as shown in Scheme 1. The nitration of *2* (path A) proceeds faster than the oxidation of *2*. In path A, 3, 4, and 5 formed are rapidly oxidized to yield dinitropyrenediones ($MW=322$), which are rapidly oxidized to give 9 and 10 ($MW=336$). Although small amounts of 3, 4, and 5 were observed under weak light irradiation ($T=21\%$ and $T=48\%$), photosensitive dinitropyrenediones would not be observed as intermediates. In path B, *2*, which is less photosensitive than 3, 4, and 5, would form 6, 7, and 8 ($MW=291$) via nitropyrenediones ($MW=277$). Photosensitive nitropyrenediones would not be observed as intermediates.

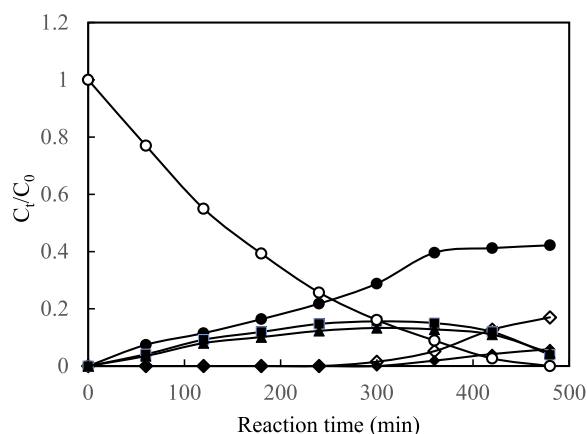
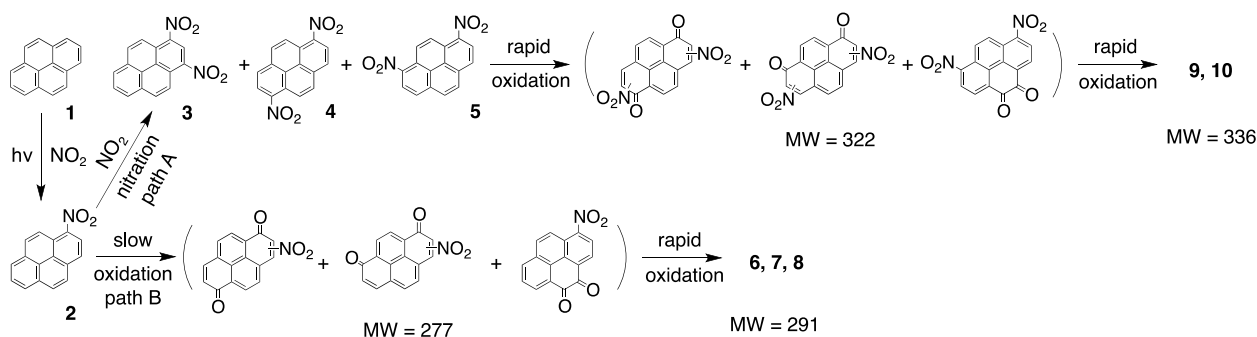


Fig. 4 Time course of the products obtained under the irradiation of the HP-Hg lamp ($T=100\%$). 10.2 ppm NO_2 in N_2 . O: pyrene, ●: 2 (1-nitropyrene), ■, ▲: 9 and 10 (photooxidation products of dinitropyrenes), ◆: 6, 7 (photooxidation products of 1-nitropyrene), ◇: 8 (photooxidation products of 1-nitropyrene)

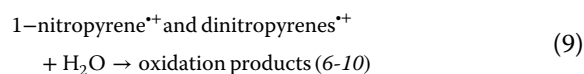
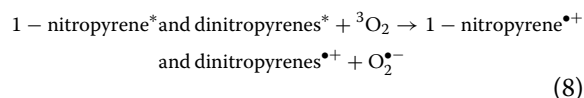
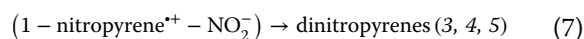
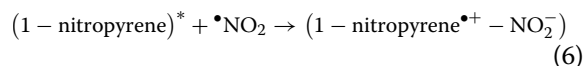
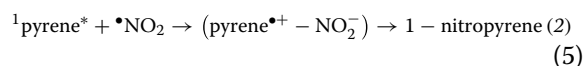
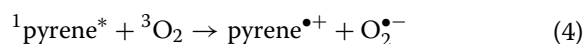
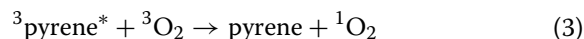
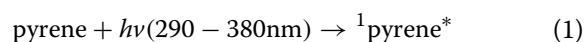
Subtracting the sum of the C_t/C_0 of 2, 6, 7, 8, 9, and 10 at 480 min from 1, the mass balance was 74%. Guan et al. (2017) reported that 1-nitropyrene photolyzes on soot to yield HNO_2 and NO . We reported that large amounts of HNO_3 ($24 \mu\text{mol g}^{-1}$) and HNO_2 (approximately $11 \mu\text{mol g}^{-1}$) were formed on silica gel by exposing 9.77 ppm NO_2 for 480 min to pyrene-adsorbed silica gel ($4.95 \mu\text{mol g}^{-1}$) without photoirradiation (Hasegawa et al. 2020; Wang et al. 2000). The experiment to determine the much less amounts of volatile HNO_2 , which could be formed by the photodecomposition of 2 and 6–10, did not give reliable results. Although the photodecomposition of 2–10 to gaseous organic products is also conceivable, as reported for pyrene on Al_2O_3 (Romanias et al. 2014), their measurements involved in the NO_2 effluent were not performed.

3.5 Photonitration mechanism

The following reaction mechanism is proposed to explain the photonitration of pyrene with NO_2 .



Scheme 1 Photonitration path of pyrene



Pyrene absorbs light in the range of 290–380 nm to produce a singlet state (${}^1\text{pyrene}^*$) of pyrene (Eq. 1). When the diluent of NO_2 was changed from N_2 to air, the energy transfer from ${}^1\text{pyrene}^*$ to ${}^3\text{O}_2$ occurred via the intersystem crossing (ISC) of ${}^1\text{pyrene}^*$ to the triplet state (${}^3\text{pyrene}^*$) of pyrene (Eqs. 2 and 3). The decrease in the concentration of ${}^1\text{pyrene}^*$ can explain the inhibition effect of oxygen on the pyrene decay, as shown in Fig. S5. On the other hand, a pyrene radical cation ($\text{pyrene}^{\bullet+}$) would be formed by the electron transfer from ${}^1\text{pyrene}^*$ to ${}^3\text{O}_2$ (Eq. 4). Equations 2–4 can be also supported by the photolysis mechanism of pyrene adsorbed on alumina (Pankasem & Thomas, 1991), silica (Mao & Thomas, 1995; Reyes et al., 2000), and KNO_3 films (Ammar et al., 2010).

The addition of $\cdot\text{NO}_2$ to ${}^1\text{pyrene}^*$ would generate the intermediate ($\text{pyrene}^{\cdot+}\text{-NO}_2^-$), which is followed by the formation of 1-nitropyrene (Eq. 5). Since the concentration of exposed $\cdot\text{NO}_2$ is constant and the concentration of ${}^1\text{pyrene}^*$ is considered to be in a steady state depending on the NO_2 diluents, we deduce that pyrene decayed according to the following pseudo-first-order kinetics.

$$-d[\text{pyrene}]/dt = k_{\text{obs}}[\text{pyrene}] \quad (10)$$

Dinitropyrenes (3, 4, 5) would be formed via intermediate ($1\text{-nitropyrene}^{\cdot+}\text{-NO}_2^-$), which was formed by the addition of $\cdot\text{NO}_2$ to the 3, 6, and 8 carbon atoms of the pyrene ring (Eqs. 6 and 7). As 1-nitropyrene and dinitropyrenes have a wide absorption band at 320–440 nm, they can absorb the emission lines (365 and 436 nm) from the HP-Hg lamp. Ammar et al. (2010) studied the photoenhanced conversion of NO_2 on pyrene/ KNO_3 films to HNO_2 , NO , NO_2^- , and traces of 1-nitropyrene and postulated the species of ($\text{pyrene}^{\cdot+}\text{-NO}_2^-$), which is formed by the reaction of pyrene^* with NO_2 . Brigante et al. (2008) also suggested a nitration mechanism via radical cations for the reaction of NO_2 with pyrene films. We considered that the radical cation intermediate ($\text{pyrene}^{\cdot+}\text{-NO}_2^-$) proposed by Ammar et al. (2010) would also act in the photonitration of pyrene. It has been reported that $\cdot\text{NO}_2$ generated by the photoirradiation of oxygenated 1-nitronaphthalene + $\text{NO}_2^-/\text{HNO}_2$ (Madigapu et al., 2011) and phenol + $\text{NO}_3^-/\text{NO}_2^-$ solutions (Vione et al., 2001, 2005; Bedini et al., 2012) would react with excited 1-nitronaphthalene and phenol to yield dinitronaphthalene and nitrophenol isomers via the addition of $\cdot\text{NO}_2$ to 1-nitronaphthalene* and phenol* and subsequent H-atom abstraction by oxygen. At present, we consider that the radical cation mechanism is more probable than the NO_2 addition mechanism because the formation of the radical cation supports the formation of photooxidation products (Ammar et al., 2010).

The photooxidation products (6–10) would be formed by the reaction of the radical cations of 2–5 with water adsorbed on silica gel (Eq. 9) as reported for the photolysis of pyrene on silica gel (Reyes et al. 2000). The origin of the O_2 for the formation of the radical cations can be illustrated by the following reports. Mao and Thomas (1994) reported that the photoirradiation of degassed pyrene on silica gel induced an electron transfer showing $\text{pyrene}^{\cdot+}$. They also reported that adsorbed oxygen on silica gel served as an electron trap of excited pyrene to form $\text{O}_2^{\cdot-}$ and $\text{pyrene}^{\cdot+}$. Reyes et al. (2000) reported that the photoexcitation of pyrene adsorbed on air-saturated silica gel produced $\text{pyrene}^{\cdot+}$ under N_2 . As pyrene-adsorbed silica gel is saturated with air in our experiment, the photooxidation products (6–10) would be produced under the N_2 diluent.

3.6 Photonitration of pyrene with low concentration NO_2

Figure 5a–d shows the time courses of the photonitration of pyrene with NO_2 under the photonitration conditions of (b) and (c), in which the concentration ratio of NO_2 to $\text{pyrene}_{\text{ads}}$ is kept constant, with nitration in the dark and the photolysis of pyrene under N_2 and air diluents. The concentrations of NO_2 and $\text{pyrene}_{\text{ads}}$ are shown on the tops of Fig. 5a–d. The time courses of pyrene and the products were determined via HPLC measurements. The products extracted after 24, 48, and 60 h were analyzed via GC-MS measurement, and the yields were estimated by comparing their GC peak areas.

Under 2.0-ppm NO_2 in N_2 (Fig. 5a), 98.4% of pyrene decayed for 24 h, which is three times longer than 8 h under 10.2-ppm NO_2 , according to the pseudo-first-order kinetics. The yields of 2 (21.6%) and 8–10 (8.0%) for 24 h were lower than those of 2 (42.2%) and 6–10 (31.4%) produced for 8 h under 10.2-ppm NO_2 (Fig. 4), suggesting that 2 and 8–10 could be easily photodecomposed when $\text{pyrene}_{\text{ads}}$ decreased from $950 \text{ pg } \mu\text{g}^{-1}$ (coverage: 0.0067) to $184 \text{ pg } \mu\text{g}^{-1}$ (coverage: 0.0013). Under 2.0-ppm NO_2 in air (Fig. 5b), the decay rate of pyrene was decreased by the inhibition effect of oxygen, resulting in a further decrease in the yields of 2 (4.9%) and 6–10 (3.8%) for 24 h. The photolysis rate of pyrene increased by 4.8 times that in 10.2-ppm NO_2 for 8 h. Fifty-six percent of the pyrene, of which 24% decayed due to photolysis for 24 h, decayed according to near the pseudo-first-order kinetics. Small amounts of 1,6-pyrenedione ($MW=232$, 0.4% in N_2 and 0.2% in air), which were identified by matching the retention time and mass spectrum with those of a standard sample, and two unidentified-structure products ($MW=230$ and 246, 0.6% in N_2) also formed. In the dark, the sigmoid curves of the decay of 1 and the formation of 2 were very similar in Fig. 5a and b and even replaced N_2 in the dilution gas with air because they were not influenced by the oxygen concentration in the dark reaction.

Under 0.20-ppm NO_2 in N_2 (Fig. 5c), 89% of pyrene, of which 27% decayed due to photolysis, decayed for 24 h according to near the pseudo-first-order kinetics. The decay curve of pyrene appears to deviate downward from the first-order decay after 12 h because it involves the decay by its own photolysis. The yields of 2 and 8 were 2.3% and 3.4% for 24 h, respectively. Under 0.20-ppm NO_2 in air (Fig. 5d), the decay of pyrene was inhibited by oxygen in the air. Sixty percent of pyrene, of which 40% decayed due to photolysis, decayed for 24 h according to near the pseudo-first-order kinetics. The decay curve of pyrene appears to deviate downward from the first-order decay after 12 h because it involves the decay by own photolysis. The yields of 2 and 8 for 24 h were 2.1% and

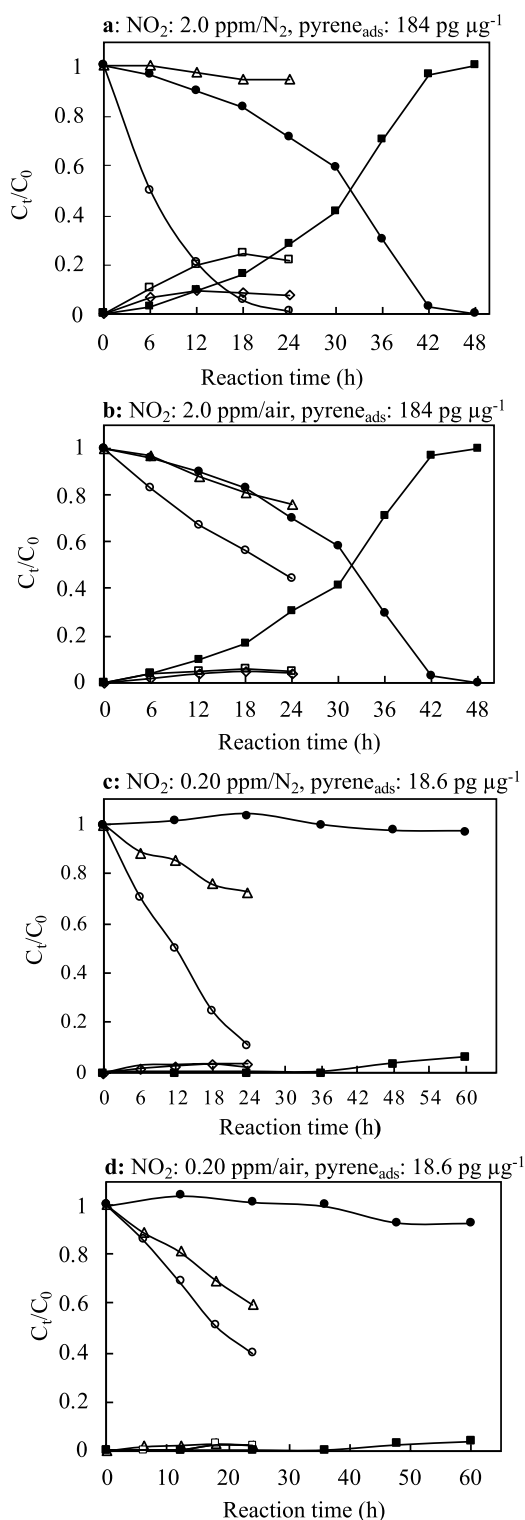


Fig. 5 Nitration of pyrene with 2.0 and 0.20 ppm NO_2 under the HP-Hg lamp ($T=100\%$) (\square , \square , \diamond) and in the dark (\bullet , \blacksquare) and photolysis of pyrene in the absence of NO_2 (\triangle). \circ , \bullet : 1 (pyrene), \square , \blacksquare : 2 (1-nitropyrene), \diamond : 8–10 (photooxidation products)

0.9%, respectively. In the dark, the yields of 2 in N_2 and air diluents for 60 h were 6.0% and 4.0%, respectively.

Figure S9 summarizes the concentration changes in pyrene by exposure to 10.2, 2.0, and 0.20 ppm NO_2 in N_2 or air diluent. Under 10.2- and 2.0-ppm NO_2 in N_2 , the decay rate of pyrene decreased according to the pseudo-first-order reaction shown in Eq. 10, and the half-lives of pyrene decay were estimated to be 1.8 h under 10.2-ppm NO_2 and 6.0 h under 2.0-ppm NO_2 . Under 2.0-ppm NO_2 in air, the half-life was estimated to be 20.9 h. Under 0.20-ppm NO_2 , the half-lives were estimated to be 12.0 h in N_2 and 18.2 h in air. If the NO_2 concentration is diluted tenfold from 2.0 to 0.20 ppm under constant $\text{pyrene}_{\text{ads}}$ of $184 \text{ pg } \mu\text{g}^{-1}$, the pyrene decay rate under 0.20-ppm NO_2 should be significantly decreased, resulting in the significant extension of its half-life. However, in N_2 diluent, the half-life under 0.20-ppm NO_2 was 2.0 times longer than that under 2.0-ppm NO_2 , and in air diluent, it was 0.87 times shorter than that under 2.0-ppm NO_2 . These results can be explained by the following two reasons. First, the concentration of $\text{pyrene}_{\text{ads}}$ was set to be proportional to the NO_2 concentration because the concentrations of NO_2 and $\text{pyrene}_{\text{ads}}$ on heavy traffic road are considered to be positively correlated. Second, the photodecomposition of pyrene was easily occurred with the decrease in the concentration of NO_2 and in the presence of air. Therefore, the photonitration of pyrene under 0.20-ppm NO_2 proceeded faster than that expected from the dilution ratio of NO_2 .

Romanias et al. (2014) have reported that gaseous products are formed by the photodegradation of pyrene on Al_2O_3 in the presence of oxygen. It has been reported that 1-nitropyrene formed on soot is photolyzed with the formation of HNO_2 and NO (Guan et al., 2017), and it is also photolyzed to form HNO_2 and NO with the consumption of nitro groups and the formation of aromatic $\text{C}=\text{O}$ groups and phenolic hydroxyls (You et al., 2022). Attempts to confirm the photodecomposition products were hitherto unsuccessful. Repeated experiments are necessary to examine the variability of the measurement due to low concentrations of NO_2 and $\text{pyrene}_{\text{ads}}$.

4 Conclusions

The photonitration of pyrene adsorbed on silica gel with NO_2 (10.2, 2.0, and 0.20 ppm in N_2 or air) was studied. Under 10.2- and 2.0-ppm NO_2 in N_2 and air, the concentration of pyrene decreased exponentially in accordance with the pseudo-first-order reaction under UV-light irradiation, while in the dark, it decreased sigmoidally in accordance with the H^+ -autocatalyzed reaction. Nitration products, their photooxidation products, and both

time profiles were examined under 10.2 ppm NO₂ in N₂. The yields of formed 1-nitropyrene and minor dinitropyrenes were decreased by the transformation into their photooxidation products. The yield of 1-nitropyrene was 42% in N₂ and 28% in air for 8 h. The inhibition effect of oxygen can be explained by the energy transfer from ¹pyrene* to oxygen. Radical cation intermediate (pyrene^{•+}-NO₂⁻) was proposed for 1-nitropyrene formation. Under 24-h exposure of pyrene to 2.0-ppm NO₂, the yields of 1-nitropyrene and the photooxidation products were 21.6% and 8.0%, respectively, in N₂ and 4.9% and 3.8%, respectively, in air. In the photonitration of pyrene under 0.20-ppm NO₂, the photolysis of pyrene concomitantly occurred especially in air diluent. Under 24-h exposure of pyrene to 0.20-ppm NO₂, the yields of 1-nitropyrene and the photooxidation products were 2.3% and 3.4%, respectively, in N₂ and 2.1% and 0.9%, respectively, in air. The significant decrease in the yields of 1-nitropyrene and the photooxidation products under the concentration of 0.20-ppm NO₂ can be explained by their easy photodecomposition with the increase in the photolysis of pyrene. Under the concentration of 0.20-ppm NO₂ in air, which is approximately the concentration on heavy-traffic roads, the decay rate of pyrene by the photonitration was increased by own photolysis, although the photonitration was inhibited by oxygen in air. Further studies are necessary to identify the correct structures of the photooxidation products and to examine the photodecomposition products of the nitration and the photooxidation products.

Supplementary Information

The online version contains supplementary material available at <https://doi.org/10.1007/s44273-023-00006-9>.

Additional file 1: Fig. S1. Fluidized-bed reaction apparatus. Fig. S2. Relationship between $\ln(C_f/C_0)$ and reaction time under the irradiation (T = 100%) of the HP-Hg lamp. 10.2 ppm NO₂ in N₂. Fig. S3. Effect of wavelength on the nitration of pyrene with NO₂ (10.2 ppm in N₂) under the irradiation of the UHP-Hg lamp. ●: $\lambda = 300\text{--}380\text{ nm}$, UV35: 14.43 mW cm⁻²; ■: $\lambda > 370\text{ nm}$, UV42: 5.03 mW cm⁻². Flow rate of NO₂: 200 mL min⁻¹. Fig. S4. Relationship between $\ln(C_f/C_0)$ and reaction time under the irradiation of 300–380 nm. 10.2 ppm NO₂ in N₂. UV35: 14.43 mW cm⁻². Fig. S5. (a): Effect of the oxygen concentration in dilution gas on the reaction of pyrene with NO₂ (10.2 ppm) under the UHP-Hg lamp. ●: [O₂] = 0% (N₂), ▲: [O₂] = 21% (air), flow rate = 200 mL min⁻¹, $\lambda = 300\text{--}380\text{ nm}$, UV35: 14.5 mW cm⁻². (b): Stern-Volmer plots of fluorescence quenching of pyrene in acetonitrile. ●: [O₂] = 0% (N₂), 21% (air), 50%, and 100%, pyrene: 10 μM, $\lambda_{ex} = 335\text{ nm}$, $\lambda_{em} = 375\text{ nm}$. Fig. S6. Relationship between $\ln(C_f/C_0)$ and reaction time under N₂ (●) and air (■) diluents of NO₂. Fig. S7. HPLC chromatograms of the extracts obtained under the irradiation of the HP-Hg lamp (T = 21%). 10.2 ppm NO₂ in N₂. Fig. S8. HPLC chromatograms of the extracts obtained under the irradiation of the HP-Hg lamp (T = 100%). 10.2 ppm NO₂ in N₂. Fig. S9. Concentration changes in pyrene by exposure to 10.2, 2.0, and 0.20 ppm NO₂ in N₂ or air diluent. HP-Hg lamp, T = 100%. O: Fig. 1 (10.2 ppm NO₂ in N₂), □: Fig. 5a (2.0 ppm NO₂ in N₂), △: Fig. 5c (0.20 ppm NO₂ in N₂), ■: Fig. 5b (2.0 ppm NO₂ in air), ▲: Fig. 5d (0.20 ppm NO₂ in air).

Acknowledgements

We thank Miss Misao Shinoda for GC-MS measurement. This work was supported by the Steel Foundation for Environmental Protection Technology (No. 12-13SR1-126).

Authors' contributions

Kiyoshi Hasegawa: Conceptualization, Methodology, Discussion, Writing of manuscript, review & editing. Reona Mabuchi: Experiment, Validation, Visualization, Discussion. Shigehiro Kagaya: Validation, Visualization, discussion, review & editing.

Declarations

Competing interests

The authors declare that they have no competing interests.

Accepted: 6 June 2023

Published online: 01 August 2023

References

- Ammar, R., Monge, M. E., George, C., & D'Anna, B. (2010). Photoenhanced NO₂ loss on simulated urban grime. *ChemPhysChem*, 11, 3956–3961.
- Barbas, J. T., Sigman, M. E., Buchanan, A. C., III, & Chevis, E. A. (1993). Photolysis of substituted naphthalenes on SiO₂ and Al₂O₃. *Photochemistry and Photobiology*, 58, 155–158.
- Bedini, A., Maurino, V., Minero, C., & Vione, D. (2012). Theoretical and experimental evidence of the photonitration pathway of phenol and 4-chlorophenol: A mechanistic study of environmental significance. *Photochemical & Photobiological Sciences*, 11, 418–424.
- Brigante, M., Cazor, D., D'Anna, B., George, C., & Donaldson, D. J. (2008). Photoenhanced uptake of NO₂ by pyrene solid films. *Journal of Physical Chemistry A*, 112, 9503–9508.
- Cochran, R. E., Jeong, H., Haddadi, S., Derseh, R. F., Gowan, A., Beranek, J., & Kubatova, A. (2016). Identification of products formed during the heterogeneous nitration and ozonation of polycyclic aromatic hydrocarbons. *Atmospheric Environment*, 128, 92–103.
- Figuren-Fernandez, A., Miguel, A. H., Lu, R., Purvis, K., Grant, B., Mayo, P., Stefano, E. D., Cho, A. K., & Froines, J. (2008). Atmospheric formation of 9,10-phenanthraquinone in the Los Angeles air basin. *Atmospheric Environment*, 42, 2312–2319.
- Gao, J., Tian, H., Cheng, K., Lu, L., Zheng, M., Wang, S., Hao, J., Wang, K., Hua, S., Zhu, C., & Wang, Y. (2015). The variation of chemical characteristics of PM_{2.5} and PM₁₀ and formation causes during two haze pollution events in urban Beijing, China. *Atmospheric Environment*, 107, 1–8.
- Garcia-Berrios, Z. I., & Arce, R. (2012). Photodegradation mechanisms of 1-nitropyrene, an environmental pollutant: The effect of organic solvents, water, oxygen, phenols, and polycyclic aromatics on the destruction and product yields. *The Journal of Physical Chemistry A*, 116, 3652–3664.
- Guan, C., Li, X., Zhang, W., & Huang, Z. (2017). Identification of nitration products during heterogeneous reaction of NO₂ on soot in the dark and under simulated sunlight. *The Journal of Physical Chemistry A*, 121, 482–492.
- Harrison, R. M., & Yin, J. (2000). (2000) Particulate matter in the atmosphere: Which particle properties are important for its effects on health? *The Science of the Total Environment*, 249, 85–101.
- Hasegawa, K., Kanbara, T., & Kagaya, S. (1998). Photocatalyzed degradation of agrochemicals in TiO₂ aqueous suspensions. *Denki Kagaku Oyoobi Kogyo Butsuri Kagaku*, 66, 625–634.
- Hasegawa, K., Takanami, T., Kawai, T., & Kagaya, S. (2020). Effects of adsorbed water and hydrocarbon reactivity on the nitration of polycyclic aromatic hydrocarbons adsorbed on silica gel and Fe₂O₃ particles with NO₂. *Atmospheric Environment*, 236, 117641.
- Inazu, K., Kobayashi, T., & Hisamatsu, Y. (1997). Formation of 2-nitrofluoranthene in gas-solid heterogeneous photoreaction of fluoranthene supported on oxide particles in the presence of nitrogen dioxide. *Chemosphere*, 35, 607–622.

- Kameda, T., Akiyama, A., Toriba, A., Tang, N., & Hayakawa, K. (2011). Atmospheric formation of hydroxynitropyrenes from a photochemical reaction of particle-associated 1-nitropyrene. *Environmental Science & Technology*, *45*, 3325–3332.
- Kameda, T., Azumi, E., Fukushima, A., Tang, N., Matsuki, A., Kamiya, Y., Toriba, A., & Hayakawa, K. (2016). Mineral dust aerosols promote the formation of toxic nitropolycyclic aromatic compounds. *Scientific Reports*, *6*, 24427.
- Keyte, I. J., Harrison, R. M., & Lammel, G. (2013). Chemical reactivity and long-range transport potential of polycyclic aromatic hydrocarbons – A review. *Chemical Society Reviews*, *42*, 9333–9391.
- Kojima, Y., Inazu, K., Hisamatsu, Y., & Okochi, H. (2010). Influence of secondary formation on atmospheric occurrences of oxygenated polycyclic aromatic hydrocarbons in airborne particles. *Atmospheric Environment*, *44*, 2873–2880.
- Lin, Y., Ma, Y., Qiu, X., Li, R., Fang, Y., Wang, J., Zhu, Y., & Hu, D. (2015). Sources, transformation, and health implications of PAHs and their nitrated, hydroxylated, and oxygenated derivatives in PM_{2.5} in Beijing. *Journal of Geophysical Research: Atmospheres*, *120*, 7219–7228.
- Liu, S. V., Chen, F.-L., & Xue, J. (2019). A meta-analysis of selected near-road air pollutants based on concentration decay rates. *Heliyon*, *5*, e02236.
- Ma, J., Liu, Y., & He, H. (2011). Heterogeneous reactions between NO₂ and anthracene adsorbed on SiO₂ and MgO. *Atmospheric Environment*, *45*, 917–924.
- Ma, Y., Cheng, Y., Qiu, X., Lin, Y., Cao, J., & Hu, D. (2016). A quantitative assessment of source contributions to fine particulate matter (PM_{2.5})-bound polycyclic aromatic hydrocarbons (PAHs) and their nitrated and hydroxylated derivatives in Hong Kong. *Environmental Pollution*, *219*, 742–749.
- Maddigapu, P. R., Minero, C., Maurino, V., Vione, D., Brigante, M., Charbouillot, T., Sarakha, M., & Mailhot, G. (2011). Photochemical and photosensitized reactions involving 1-nitronaphthalene and nitrite in aqueous solution. *Photochemical & Photobiological Sciences*, *10*, 601–609.
- Mao, Y., & Thomas, J. K. (1994). Reactions of electrons generated in photolysis of pyrene on silica gel surfaces. *Chemical Physics Letters*, *226*, 127–131.
- Mao, Y., & Thomas, J. K. (1995). Chemical reactions of molecular oxygen in surface-mediated photolysis of aromatic compounds on silica-based surfaces. *The Journal of Physical Chemistry*, *99*, 2048–2056.
- Miet, K., Menach, K. L., Flaud, P.-M., Budzinski, H., & Villenave, E. (2009). Heterogeneous reactivity of pyrene and 1-nitropyrene with NO₂: Kinetics, product yields and mechanism. *Atmospheric Environment*, *43*, 837–843.
- Pankasem, S., & Thomas, J. K. (1991). Reflectance spectroscopic studies of the cation radical and the triplet of pyrene on alumina. *The Journal of Physical Chemistry*, *95*, 6990–6996.
- Perraudin, E., Budzinski, H., & Villenave, E. (2005). Kinetic study of the reactions of NO₂ with polycyclic aromatic hydrocarbons adsorbed on silica particles. *Atmospheric Environment*, *39*, 6557–6567.
- Reyes, C. A., Medina, M., Crespo-Hernandez, C., Cedeno, M. Z., Arce, R., Rosario, O., Steffenson, D. M., Ivanov, I. N., Sigman, M. E., & Dabestani, R. (2000). Photochemistry of pyrene on unactivated and activated silica surfaces. *Environmental Science & Technology*, *34*, 415–421.
- Rodriguez, I., Gali, S., & Marcos, C. (2009). Atmospheric inorganic aerosol of a non-industrial city in the centre of an industrial region of the North of Spain, and its possible influence on the climate on a regional scale. *Environmental Geology*, *56*, 1551–1561.
- Romanias, M. N., Andrade-Eiroa, A., Shahla, R., Bedjanian, Y., Zogka, A. G., Philippidis, A., & Dagaut, P. (2014). Photodegradation of pyrene on Al₂O₃ surfaces: A detailed kinetic and product study. *The Journal of Physical Chemistry A*, *118*, 7007–7016.
- Saltzman, B. E. (1960). Modified nitrogen dioxide reagent for recording air analyzers. *Analytical Chemistry*, *32*, 135–136.
- Sugiyama, H., Watanabe, T., & Hirayama, T. (2001). Nitration of pyrene in metallic oxides as soil components in the presence of indoor air, nitrogen dioxide gas, nitrite ion, or nitrate ion under xenon irradiation. *Journal of Health Science*, *47*, 28–35.
- Tang, N., Hakamata, M., Sato, K., Okada, Y., Yang, X., Tatsumatsu, M., Toriba, A., Kameda, T., & Hayakawa, K. (2015). Atmospheric behaviors of polycyclic aromatic hydrocarbons at a Japanese remote background site, Noto peninsula, from 2004 to 2014. *Atmospheric Environment*, *120*, 144–151.
- United States Environmental Protection Agency (U. S. EPA). (2011). Air quality guide for nitrogen dioxide. <https://www.airnow.gov/sites/default/files/2018-06/no2.pdf> (2023/2/18).
- Vione, D., Maurino, V., Minero, C., & Pelizzetti, E. (2001). Phenol photolysis upon UV irradiation of nitrate in aqueous solution I: (2001) Effect of oxygen and 2-propanol. *Chemosphere*, *45*, 893–902.
- Vione, D., Maurino, V., Minero, C., & Pelizzetti, E. (2005). Aqueous atmospheric chemistry: Formation of 2,4-dinitrophenol upon nitration of 2-nitrophenol and 4-nitrophenol in solution. *Environmental Science & Technology*, *39*, 7921–7931.
- Wang, H., Hasegawa, K., & Kagaya, S. (1999). Nitration of pyrene adsorbed on silica particles by nitrogen dioxide under simulated atmospheric conditions. *Chemosphere*, *39*, 1923–1936.
- Wang, H., Hasegawa, K., & Kagaya, S. (2000). The nitration of pyrene adsorbed on silica particles by nitrogen dioxide. *Chemosphere*, *41*, 1479–1484.
- Wu, C.-H., & Niki, H. (1985). Fluorescence spectroscopic study of kinetics of gas-surface reactions between nitrogen dioxide and adsorbed pyrene. *Environmental Science & Technology*, *19*, 1089–1094.
- You, D., Yang, W., Xu, W., Yan, R., & Han, C. (2022). Photolysis of 1-nitropyrene: HONO and NO formations, optical property changes and mechanism insights. *Atmospheric Environment*, *272*, 118925.
- Zhuo, S., Du, W., Shen, G., Li, B., Liu, J., Cheng, H., Xing, B., & Tao, S. (2017). Estimating relative contributions of primary and secondary sources of nitrated and oxygenated polycyclic aromatic hydrocarbons. *Atmospheric Environment*, *159*, 126–134.

Publisher's Note

Springer Nature remains neutral with regard to jurisdictional claims in published maps and institutional affiliations.